# European small portable rainfall simulators: A comparison of rainfall characteristics

T. Iserloh[a*], J.B. Ries[a], J. Arnáez[b], C. Boix-Fayos[c], V. Butzen[a], A. Cerdà[d], M.T. Echeverría[e], J. Fernández-Gálvez[f], W. Fister[g], C. Geißler[h], J.A. Gómez[i], H. Gómez-Macpherson[i], N.J. Kuhn[g], R. Lázaro[j], F.J. León[e], M. Martínez-Mena[c], J.F. Martínez-Murillo[k], M. Marzen[a], M.D. Mingorance[f], L. Ortigosa[b], P. Peters[l], D. Regüés[m], J.D. Ruiz-Sinoga[k], T. Scholten[h], M. Seeger[a,l], A. Solé-Benet[j], R. Wengel[a], S. Wirtz[a]

[a] *Physical Geography, Trier University, 54286 Trier, Germany*
[b] *Physical Geography, University of La Rioja, 26004 Logroño, Spain*
[c] *Soil and Water Conservation Department (CEBAS-CSIC), 30100 Murcia, Spain*
[d] *Department of Geography, University of Valencia, 46010 Valencia, Spain*
[e] *Department of Geography and Spatial Management, University of Zaragoza, 50009 Zaragoza, Spain*
[f] *Andalusian Institute for Earth Sciences (UGR-CSIC), 18100 Granada, Spain*
[g] *Physical Geography and Environmental Change, University of Basel, 4056 Basel, Switzerland*
[h] *Physical Geography and Soil Science, Eberhard Karls University Tübingen, 72070 Tübingen, Germany*
[i] *Institute for Sustainable Agriculture (IAS-CSIC), Apartado 4084, 14080 Córdoba, Spain*
[j] *Arid Zones Experimental Station (EEZA-CSIC), 04120 Almería, Spain*
[k] *Department of Geography, University of Málaga, 29079 Málaga, Spain*
[l] *Land Degradation and Development, Wageningen University,6700 Wageningen, the Netherlands*
[m] *Pyrenean Institute of Ecology (IPE-CSIC), 50059 Zaragoza, Spain*
[*] *Corresponding author: Tel.: +49-651-2013390, e-mail: iserloh@uni-trier.de, Fax: +49-651-2013976.*
*DOI: 10.1016/j.catena.2013.05.013*

**Abstract** Small-scale portable rainfall simulators are an essential research tool for investigating the process dynamics of soil erosion and surface hydrology. There is no standardisation of rainfall simulation and such rainfall simulators differ in design, rainfall intensities, rain spectra and research questions, which impede drawing a meaningful comparison between results. Nevertheless, these data become progressively important for soil erosion assessment and therefore, the basis for decision-makers in application-oriented erosion protection.

The artificially generated rainfall of the simulators used at the Universities Basel, La Rioja, Malaga, Trier, Tübingen, Valencia, Wageningen, Zaragoza, and at different CSIC (Spanish Scientific Research Council) institutes (Almeria, Cordoba, Granada, Murcia and Zaragoza) was measured with the same methods (Laser Precipitation Monitor for drop spectra and rain collectors for spatial distribution). Data are very beneficial for improvements of simulators and comparison of simulators and results. Furthermore, they can be used for comparative studies, e.g. with measured natural rainfall spectra. A broad range of rainfall data was measured (e.g. intensity: 37 – 360 mm $h^{-1}$; Christiansen Coefficient for spatial rainfall distribution: 61 – 98 %; median volumetric drop diameter: 0.375 – 6.5 mm; mean kinetic

energy expenditure: 25 – 1322 J $m^{-2}$ $h^{-1}$; mean kinetic energy per unit area and unit depth of rainfall: 0.77 – 50 J $m^{-2}$ $mm^{-1}$). Similarities among the simulators could be found e.g. concerning drop size distributions (maximum drop numbers are reached within the smallest drop classes < 1 mm) and low fall velocities of bigger drops due to a general physical restriction. The comparison represents a good data-base for improvements and provides a consistent picture of the different parameters of the simulators that were tested.

*Keywords:*
Rainfall simulator comparison; Runoff; Drop size; Drop velocity; Kinetic energy; Spatial rainfall distribution; Water erosion

## 1. Introduction

Rainfall simulation has become an important method for assessing the subjects of soil erosion and soil hydrological processes. It is an essential tool for investigating the different erosion processes *in situ* and in the laboratory, particularly for quantifying rates of detachment and transportation of material (e.g. Cerdà, 1999). Its application allows a quick, specific and reproducible assessment of the meaning and impact of several factors, such as slope, soil type (infiltration, permeability), soil moisture, splash effect of raindrops (aggregate stability), surface structure, vegetation cover and vegetation structure (Bowyer-Bower and Burt, 1989; Schmidt, 1998). The possibility of high repetition rate offers a systematic approach to address the different factors that influence soil erosion even in remote areas and in regions where highly erosive rainfall events are rare or irregular. A compilation of different rainfall simulator systems is given by Meyer (1988) and Hudson (1995). Cerdà (1999) reports on the history of rainfall simulation over the past 62 years and lists 229 different simulators by author, year of construction, application by country, nozzle type, capillary material, drop diameter, precipitation intensity, plot size and research question.

The need to distinguish the different partial processes of runoff generation and erosion led to the development of rainfall simulations on small plots (Calvo et al., 1988). The advantages of

small portable rainfall simulators are, among others, the low costs, the easy transport in inaccessible areas and the low water consumption. Small portable rainfall simulators also enable data to be obtained under controlled conditions and over relatively short time periods. They have been used worldwide by different research groups for many years. Since 1938 more than 100 rainfall simulators with plot dimensions <5 m² (most of them <1 m²) were developed (e.g. Abudi et al., 2012; Adams et al., 1957; Alves Sobrinho et al., 2008; Battany and Grismer, 2000; Birt et al., 2007; Blanquies et al., 2003; Bork, 1981; Bryan, 1974; Calvo et al., 1988; Cerdà et al., 1997; Clarke and Walsh, 2007; Farres, 1987; Hudson, 1965; Humphry et al., 2002; Imeson, 1977; Kamphorst, 1987; Loch et al., 2001; Luk, 1985; Martínez-Mena et al., 2001a; Medalus, 1993; Nadal-Romero and Regüés, 2009; Neal, 1937; Norton, 1987; De Ploey, 1981; Poesen et al., 1990; Regmi and Thompson, 2000; Regüés and Gallart, 2004; Roth et al., 1985; Torri et al., 1999; Wilm, 1943). There is no standardisation of rainfall simulation and these rainfall simulators differ in design, rainfall intensities, spatial rainfall distribution, drop sizes and drop velocities, which impede drawing a meaningful comparison between results. Nevertheless, the data have become progressively important for soil erosion assessment and decision-making in application-oriented erosion protection. Therefore, the accurate knowledge of test conditions is a fundamental requirement and is essential to interpret, combine and classify results (Boulal et al., 2011; Clarke and Walsh, 2007; Lascelles et al., 2000; Ries et al., 2013).

A summary of major requirements for small portable rainfall simulators is given in Iserloh et al. (2012). The most substantial and critical properties of a simulated rainfall are the drop size distribution (DSD), the fall velocities of the drops and the spatial distribution of the rainfall on the plot-area. Since the 1970s, published studies have shown variations in these properties generated by respective simulators (e.g. Cerdà et al., 1997; Fister et al., 2011, 2012; Hall, 1970; Hassel and Richter, 1988; Humphry et al., 2002; Iserloh et al., 2012; Kincaid et al., 1996; King et al., 2010; Lascelles et al., 2000; Ries et al., 2009; Salles et al., 1999; Zhao et al., 1996). Many techniques were used to characterise simulated rainfall, such as the flour pellet method (Hudson, 1963; Laws and Parsons, 1943), laser particle measuring system (Salles and Poesen, 1999; Salles et al., 1999), plaster micro plot (Ries and Langer, 2001), indication paper (Brandt,

1989; Cerdà et al., 1997; Salles et al., 1999; Wiesner, 1895), Joss-Waldvogel Disdrometer (Hassel and Richter, 1988; Joss and Waldvogel, 1967) and the oil method (Gunn and Kinzer, 1949) among others. It was shown that the results of the characterisation of simulated rainfall were extremely dependent on the particular method that was applied (Ries et al., 2009). Against this backdrop, a standardized method for verifying and calibrating the characteristics of simulated rainfall is paramount, and the Laser Precipitation Monitor (LPM) represents the most up-to-date and accurate measurement technique for obtaining information on drop spectra and drop fall velocities (King et al., 2010; Ries et al., 2009), along with an optimal price-performance ratio. Quantity and spatial distribution of the simulated rain can be easily measured with rain-collectors (covering the complete testplot) at low cost and good performance.

In this study, artificial rainfall generated by 13 rainfall simulators based in various European research institutions from Germany, the Netherlands, Spain and Switzerland was characterised using LPM and rain collectors in all simulations in order to ensure comparability of the results. The studied rainfall simulators represent most of the devices that have been used in Europe over the last decade and they present a wide range of designs, plot dimensions (0.06 m² up to 1 m²), numbers and types of nozzles and rainfall intensities. The main research question to be answered is: What are the most important differences/similarities in the suite of simulated rainfall characteristics investigated?

## 2. Material & methods

### 2.1 Rainfall simulators

The 13 small portable field rainfall simulators that were tested are shown in Fig. 1 and their main characteristics are listed in Table 1. The simulators are three new developed prototype nozzle-type simulators based at Tübingen (TU), Cordoba (CO) and Basel (BA) as well as two capillary-type simulators from Granada (GR) and Wageningen (WA). The eight other simulators are round plot nozzle-type simulators based at Almeria (AL), Malaga (MA), Murcia (MU), Trier (TR), Zaragoza-CSIC (ZAC), Valencia (VA), Zaragoza-University (ZAU) and La Rioja (LR), and their design follows Calvo et al. (1988) and Cerdà et al. (1997). This round plot

type of rainfall simulator is the most common device used in semi-arid areas in Europe, especially in Spain, and major differences typically occur in pumps, nozzles and applied intensities. Duration of all simulators is adjustable, only the WA-simulator is limited to three min, due to its compact design.

**Table 1**

The main characteristics of small scale portable rainfall simulators tested (ranked in order of plot size).

| ID | Plot size [m²] | Plot design | Falling height [m] | Nozzle / Drop formers | Water source | Details |
|---|---|---|---|---|---|---|
| TU | 1.000 | 1 m x 1 m, rectangular | 3.43 | Lechler 460.788.30 | Electric pressure pump (driven by power generator) | Iserloh et al. (2013) |
| CO | 0.700 | 1 m x 0.7 m, rectangular | 2.30 | Veejet 80.150 | Electric pressure pump (driven by power generator) | Alves Sobrinho et al. (2008) |
| BA | 0.700 | 1.34 m x 1.0 m x 0.3 m, trapezoid | 1.10 | Spraying Systems 3/8 HH 20W SQ | Electric pressure pump (driven by power generator) | Hikel et al. (2013); Iserloh et al. (2013) |
| GR | 0.250 | 0.5 m x 0.5 m, rectangular | 1.50 | 4900 capillaries per m² | Electric peristaltic pump (driven by power generator)+ Mariotte's bottle | Fernández-Gálvez et al. (2008) |
| AL | 0.283 | round | 2.00 | Hardi 4680-10E | Gasoline engine driven pressure pump | e.g. Li et al. (2011) |
| MA | 0.283 | round | 2.00 | Hardi 1553-20 | Electric pressure pump (driven by power generator) | e.g. Martínez-Murillo and Ruiz-Sinoga (2007) |
| MU | 0.283 | round | 2.00 | Lechler 402.608.30 | Gasoline engine driven pressure pump | Martínez-Mena et al. (2001b) |
| TR | 0.283 | round | 2.00 | Lechler 460.608.30 | Gasoline engine driven pump or electrical pump (driven by battery) | Iserloh et al. (2012, 2013) |
| ZAC | 0.283 | round | 2.22 | Lechler 460.688.30 | Gasoline engine driven pressure pump | Nadal-Romero and Regüés (2009); Nadal-Romero et al. (2011) |
| VA | 0.246 | round | 2.00 | Hardi 1553 12 | Gasoline engine driven pump or electrical pump (driven by battery) | Cerdà et al. (1997); Iserloh et al. (2013) |
| ZAU | 0.212 | round | 2.18 | Lechler 460.688.30 | Gasoline engine driven pressure pump | Iserloh et al. (2013); León et al. (2013) |
| LR | 0.160 | round | 2.50 | Lechler 460.608.17 | Gasoline engine driven pressure pump | Arnaez et al. (2007) |
| WA | 0.159 | 0.24 m x 0.24 m, rectangular | 0.40 | 49 capillaries | Cylindrical reservoir over capillaries | Iserloh et al. (2013); Kamphorst (1987) |

## 2.2 Methods for evaluating rainfall characteristics

### a) Drop size distribution and drop fall velocities

The Thies Laser Precipitation Monitor (LPM) was used for analysing the DSD and drop fall velocities. LPM measures the amount and intensity of rainfall and determines rain-drop size and velocity as the drops fall through a laser beam (area of 46 $cm^2$ (23 x 2 cm)). It registers individual drops with diameters ranging from 0.16 mm to 8 mm, and fall velocities ranging from 0.2 m $s^{-1}$ to 20 m $s^{-1}$, up to a maximum intensity of 250 mm $h^{-1}$ (Thies, 2004). A more detailed description of the LPM is given in Angulo-Martínez et al. (2012), Fister et al. (2012),

King et al. (2010) and Scholten et al. (2011). Because the LPM records only drop size and drop velocity classes, we used the mean value of each class to calculate kinetic energy, momentum and median volumetric drop diameter ($d_{50}$).

**b) Spatial rainfall distribution**

In order to generate quantitative information about the homogeneity and the reproducibility of rainfall, small rainfall collectors were used to measure the spatial rainfall distribution. The entire test plot was covered by collectors: square ones (56 cm²; in case of Basel: 100 cm²) for square plots and round collectors (20 cm²) for round plots (Fig 2).

## 2.3 Test procedure

A standardized test procedure was developed and performed with the simulators.

Prior to each test sequence, rainfall intensity was calibrated using the method generally applied by each group to maintain the customary rainfall conditions of their experimental work. TR and VA used a calibration plate covering the whole plot, TU used the LPM technique, and the remaining groups used rain collectors.

Water discharge of nozzles was determined using the volumetric method.

In order to analyse drop spectra with the LPM, five representative positions within the total plot area were chosen (Fig. 2). At each position, five replications at one minute measurement intervals were performed (except the WA-simulator whose design allows only a maximum duration of three minutes). Due to the bodywork of the LPM, the measurement height is 15 cm above ground.

Exposure time of collectors to rainfall during each replicate experiment was five min, and a total of three repetitions were undertaken. The individual collectors were weighed to determine spatial variations in the mass, and hence the volume of water at each location within the plot. The results were calculated as equivalent intensity values (mm $h^{-1}$) and spatially displayed. The measurement of rainfall distribution of the WA-simulator was not possible due to the compact construction of the simulator.


**Fig. 1.** The small-scale portable rainfall simulators from a) Tübingen (TU), b) Cordoba (CO), c) Basel (BA), d) Granada (GR), e) Almeria (AL), f) Malaga (MA), g) Murcia (MU), h) Trier (TR), i) Zaragoza-CSIC (ZAC), j) Valencia (VA), k) Zaragoza-University (ZAU), l) La Rioja (LR) and m) Wageningen (WA).

167

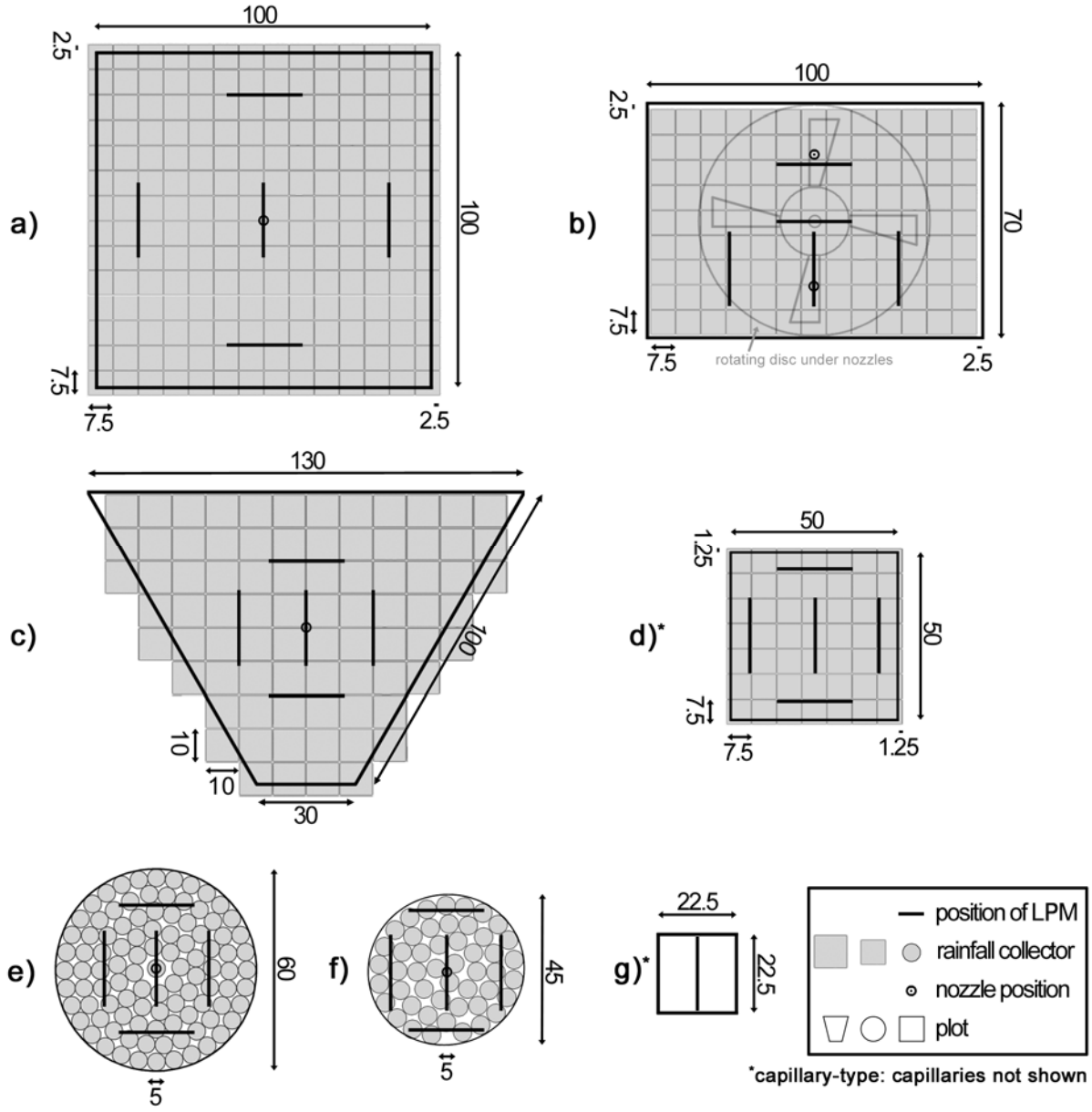


**Fig. 2.** Test set-up: a) Tübingen (TU), b) Cordoba (CO), c) Basel (BA), d) Granada (GR), e) Almeria (AL), Malaga (MA), Murcia (MU), Trier (TR), Zaragoza-CSIC (ZAC), Valencia (VA) and Zaragoza-University (ZAU), f) La Rioja (LR) and g) Wageningen (WA). LPM = Laser Precipitation Monitor.

### 2.4. Further calculations

**a) Rainfall kinetic energy and momentum**

Rainfall kinetic energy was calculated using equations from Fornis et al. (2005). These equations were provided relating to the development of the Disdrometer RD-80 (Disdromet Ltd, Basel, Switzerland, 2001) and are optimally applicable for the LPM by Thies. In order to

compute the rate of kinetic energy expenditure ($KE_R$, J m$^{-2}$ h$^{-1}$) for every 1-min period, the following equation was used:

$$KE_R = \left(\frac{\pi}{12}\right)\left(\frac{1}{10^6}\right)\left(\frac{3600}{t}\right)\left(\frac{1}{A}\right)\sum_{i=1}^{20} n_i D_i^3 \left(v_{D_i}\right)^2 \quad (1)$$

where $A$ = 0.0046 m$^2$ is the sampling area of the LPM, $n_i$ the number of drops of diameter $D_i$; $v_{D_i}$ the measured fall velocity of drop with diameter $D_i$ and $t$ = 60 s.

The kinetic energy per unit area and unit depth of rainfall, $KE$ (J m$^{-2}$ mm$^{-1}$) was calculated using equation (2):

$$KE = \left(\frac{KE_R}{I}\right) \quad (2)$$

where $I$ is the rainfall intensity (mm h$^{-1}$) measured with the LPM.

Brodie and Rosewell (2007) concluded that key processes of particle wash-off due to rainfall are slightly more dependent on momentum ($M$) than on $KE$, therefore momentum was calculated following their approach. The calculations in equation (3) were made on the basis that the momentum $M$ (kg m s$^{-1}$) of an individual raindrop of diameter $D_n$ is:

$$M_n = 10^{-3} \times m_n v_{Fn} \quad (3)$$

where $m_n$ is mass (g) of $D_n$ raindrop, $v_{Fn}$ is terminal fall velocity (m s$^{-1}$) of $D_n$ raindrop in still air.

$v_{Fn}$ is measured by the LPM, the mass, $m_n$, must be calculated (Eq. 4), and the drop volume $V_n$ (mm³) is to be determined (Eq. 5), while it is calculated from the measured drop diameters $D_n$.

$$m_n = 10^{-3} V_n \quad (4)$$

$$V_n = \frac{\pi}{6} D_n^3 \quad (5)$$

**b) Median volumetric drop diameter**

The median volumetric drop diameter ($d_{50}$) was calculated from the percentage total mass of raindrops in each size class according to Hudson (1995) and Clarke and Walsh (2007). For the calculation, the volumes of spherical drops have been assumed.

**c) Uniform Coefficient and spatial rainfall variability**

In order to compare results between different simulators, the mean Christiansen Uniformity (CU) coefficient (Christiansen, 1942) was calculated using equation (6).

$$CU = (1 - \frac{\sum_{i=1}^{n} \left| x_i - \bar{x} \right|}{\bar{x} * n}) \quad (6)$$

where $\sum_{i=1}^{n} \left| x_i - \bar{x} \right|$ is the sum of the absolute deviations from mean water amount of all rain collectors [ml], $x_i$ is individual water amount per rain collector [ml], $\bar{x}$ is the arithmetic mean of applied water amount per rain collector [ml] and n is the total number of rain collectors.

For the characterisation of spatial rainfall variability, the deviation from the mean was calculated for each collector based on the three replicate tests performed for each rainfall simulator. The deviation was then normalised by the mean rainfall intensity of the respective cell to compute a quantitative measure for the spatial reproducibility of simulated rainfall.

## 3. Results and discussion

The main rainfall characteristics for each simulator are presented in Table 2. The rainfall simulators of the participating institutes produced a broad range of intensities, from 37 mm $h^{-1}$ (MA) to 360 mm $h^{-1}$ (WA). Total water consumption per min depends on the applied intensity, the plot size and the size of nozzle used (e.g. due to different spray angles and applied water pressure). The results ranged from 0.49 L $min^{-1}$ for AL and VA, to 3.24 L $min^{-1}$ for TU. Water efficiency showed a broad data range from 4.2 % (LR: large spray angle, high water pressure) to 49.3% (AL: small spray angle, low water pressure). Particularly for those *in situ* rainfall simulator studies in (semi-) arid areas with limited water availability, water consumption should be as low and used as efficiently as possible.

**Table 2**

Main results of simulated rainfall characteristics for each rainfall simulator: water consumption, water efficiency, mean Intensity [*I*], Christiansen Uniformity [*CU*], mean spatial variability (average deviation from mean) of rainfall distribution, mean drop number [*n*], median volumetric drop diameter [$d_{50}$], mean kinetic energy expenditure [$KE_R$], mean kinetic energy per unit area per unit depth of rainfall [*KE*] and mean momentum [*M*].

| ID | Water consumption [L min$^{-1}$] | Water efficiency [%] | *I* [mm h$^{-1}$] | CU [%] | Spatial variability [%] | *n* [min$^{-1}$] | $d_{50}$ [mm] | $KE_R$ [J m$^{-2}$ h$^{-1}$] | *KE* [J m$^{-2}$ mm$^{-1}$] | *M* [kg m s$^{-1}$] |
|---|---|---|---|---|---|---|---|---|---|---|
| **TU** | 3.24 | 28.4 | 55 | 88.4 | 3.4 | 19956 | 1.25-1.75 | 475 | 9.88 | 0.0265 |
| **CO** | *a* | *a* | 67 | 81.4 | 4.4 | 19073 | 2.00-3.00 | 1322 | 13.76 | 0.0459 |
| **BA** | *a* | *a* | 43 | 87.0 | 8.9 | 18217 | 1.25-1.75 | 172 | 7.52 | 0.0132 |
| **GR** | *a* | *a* | 94 | 76.4 | 10.6 | 5640 | 4.00-5.00 | 1149 | 8.40 | 0.0518 |
| **AL** | 0.49 | 49.3 | 51 | 60.6 | 12.8 | 5094 | 2.00-3.00 | 638 | 11.51 | 0.0327 |
| **MA** | 0.48 | 36.7 | 37 | 89.3 | 5.1 | 16671 | 1.25-1.75 | 252 | 7.56 | 0.0170 |
| **MU** | 1.36 | 26.0 | 75 | 66.9 | 13.2 | 12823 | 2.00-3.00 | 355 | 7.78 | 0.0176 |
| **TR** | 0.80 | 27.0 | 46 | 90.6 | 3.8 | 19695 | 1.00-1.50 | 214 | 5.81 | 0.0157 |
| **ZAC** | 2.60 | 8.8 | 48 | 97.6 | 1.2 | 26797 | 0.50-1.00 | 77 | 3.86 | 0.0085 |
| **VA** | 0.49 | 42.9 | 51 | 86.2 | 3.5 | 8393 | 1.75-2.50 | 423 | 10.84 | 0.0244 |
| **ZAU** | 2.90 | 5.9 | 48 | 97.8 | 2.1 | 24494 | 0.50-1.00 | 54 | 4.16 | 0.0071 |
| **LR** | 2.85 | 4.2 | 45 | 96.5 | 7.9 | 20725 | 0.375-0.750 | 25 | 0.77 | 0.0042 |
| **WA** | *a* | *a* | 360 | *a* | *a* | 1190 | 5.50-6.50 | 1296 | 50.32 | 0.0917 |

[a]Not measured

## Drop spectra

The mean drop size and fall velocity measurements with the LPM are listed in Fig. 3. The major similarity is that maximum drop numbers are attained within the two smallest drop size classes <1 mm (Fig. 3 and Fig. 4): in all cases, except TU and WA, >1000 drops per min were only measured in those classes <1 mm. TU also reached 1059 drops in the drop size class 1.0-1.49 mm; the drop amounts of WA are lower than 1000 drops per min for all drop size classes. Amounts of drops >1 mm were generally much lower than that of <1 mm: max. 833 drops per min (ZAU) were measured in the drops size class 1.0-1.49 mm and a max. of

554 drops per min (AL) was detected for sizes >1.5 mm. The highest number of drops per min >2.0 mm was measured for WA (320 drops per min). More than 100 drops per min >3.0 mm were only produced by the two capillary-type simulators GR (166 drops per min) and WA (153 drops per min).

The data also show that the fall velocity of bigger drops is lower due to the general physical restriction of low drop fall heights (Fig. 3). During all simulations, 90% or more of the measured drops were slower than 3.4 m $s^{-1}$. Only TU (237 drops), CO (321 drops) and GR (158 drops) generated more than 100 drops per min with fall velocities >5 m $s^{-1}$. Drops >5.8 m $s^{-1}$ were rarely measured. A few drops with velocities around 9 m $s^{-1}$ were measured during simulations of CO, because the special water application unit in the simulator is able to accelerate bigger drops to higher fall velocities. The velocities of smaller drops (<1 mm) generated by the simulators were often similar to that expected for natural drops, as indicated by Atlas et al. (1973) and Mätzler (2002), for vertical rainfall in calm conditions. In two cases (TU and TR), more than 100 larger drops (1.0-1.49 mm) per min were accelerated to expected natural velocities.

By examining single rainfall simulators, four groups can be distinguished. During the runs of BA, ZAC, ZAU and LR, hardly any big drops (>2.5 mm) were measured. The simulators from TU, MA, MU, TR and VA produced drops >2.5 mm, but this was much less than the capillary-type simulators from GR and ZAU. The simulators from CO and AL also generated drops >2.5 mm but reached higher velocities than GR and ZAU.

Unfortunately, determining exact $d_{50}$ values for volumetric drop diameter was not possible with the LPM for two reasons. As mentioned above, the device records only size classes and not actual drop sizes, besides the fact that only drop diameters are registered. We assumed a circular form of the falling drops for our calculations (Fister et al., 2011). Nevertheless, calculation of $d_{50}$ values represents the best possible option for comparison with other rainfall simulators (Fister et al., 2012; Hudson, 1995). Hence, the lowest $d_{50}$ value of the 13 simulators was 0.375-0.750 mm (LR), and the highest was 5.5-6.5 mm (WA) (Table 2).

Most studies lack accuracy concerning calculated kinetic energy of simulated rainfall (Clarke and Walsh, 2007): the values are predominantly calculated from intensities only, based on the assumption that diameters and/or velocities from natural rainfall apply for simulated rainfall, too. Considering the general physical restrictions of simulated rainfall (e.g. fall height), we therefore assume, that most of the published data overestimate real values of kinetic energy. The *KE* values calculated in this study were maximal 56 % and minimal 3 % of the *KE* calculated with the three of the most commonly used equations for determining natural rainfall of equal intensities (van Dijk et al., 2002; Morgan et al., 1998; Wischmeier and Smith, 1978). Only the WA produced rainfall with a *KE* that was greater than that calculated for natural rainfall (up to 77 % more than calculated with each of the three mentioned equations). The high *KE* of the WA-simulator was caused by the specific characteristics (very short test duration with large, high-energy drops as described in Iserloh et al. (2013) and Kamphorst (1987).

The calculated momentums of simulated rainfalls ranged from 0.0042 kg $m^2$ $s^{-1}$ for LR up to 0.0917 kg $m^2$ $s^{-1}$ for WA. As mentioned above, some researchers concluded that key processes of particle wash off due to rainfall are slightly more dependent on momentum than on *KE* (Brodie and Rosewell, 2007). Rose (1960) found that this was the case for the rate of soil detachment per unit area, and Park et al. (1980) used a momentum power relationship to predict splash erosion (Brodie and Rosewell, 2007).

In Fig. 4 the results of the LPM measurements were plotted in relation to the drop size distribution for a hypothetical Marshall & Palmer distribution (Marshall and Palmer, 1948) of equal intensities. The box plots in Fig. 4 give additional information about the scattering of drop amounts over the 25 1-min measurement intervals on five positions. A broad scattering, reflects the heterogeneity of the spatial distribution of rainfall on the respective plot, described below.

The simulators from CO, ZAC, ZAU and LR showed little scattering in all classes, the measured values were close to the Marshall & Palmer distribution. However, in most cases there were too many drops in the 0.5-0.99 mm drop size class and too little in the 1.0-

299 1.49 mm and 1.5-1.99 mm drop size class. The simulators from TU, GR, MA, MU, TR and
300 VA showed higher scattering, especially in the small drop classes. The values were still close
301 to the Marshall-Palmer distribution. The results from the GR simulator were remarkable
302 because of the higher amount of drops >3 mm diameter. The simulators from AL and WA
303 showed deviations from the Marshall-Palmer distribution. The AL simulator produces much
304 too less drops smaller than 0.50 mm, whereas the WA simulator produces a relatively regular
305 drop size distribution over all classes.
306
307 **Spatial rainfall distribution**
308 The mean intensities based on three replicate measurements for each rain collector are
309 presented in Fig 5. Only the two simulators from Zaragoza (ZAC and ZAU) showed evenly
310 distributed intensities, caused by large spraying angles of the full cone nozzles used. All
311 other simulators showed variations over the total plot area, caused by number of applied
312 nozzles (CO) or nozzle-types as well as applied water pressure.
313 TU showed an almost uniform rainfall distribution across the whole plot (>55 mm $h^{-1}$, max.
314 68 mm $h^{-1}$) with only small patches of lower intensity values in the left upper corner and at
315 the outlet (35-55 mm $h^{-1}$). The average spatial rainfall variability over the three repetitions
316 was low, in most cases between 0 and 5%, only in few cases between 5% and 10% (Fig. 6;
317 mean values are presented in Table 2).
318 For CO, lower rainfall intensities (50-70 mm $h^{-1}$) were measured at the right and the left
319 edges of the plot, and at one strip in the middle. Higher intensities (70-97 mm $h^{-1}$) occurred
320 on the upper and the lower area of the plot. Average deviations from the mean were low, and
321 almost all collectors showed values between 0 and 10%. In one case, the value was between
322 10% and 15%.

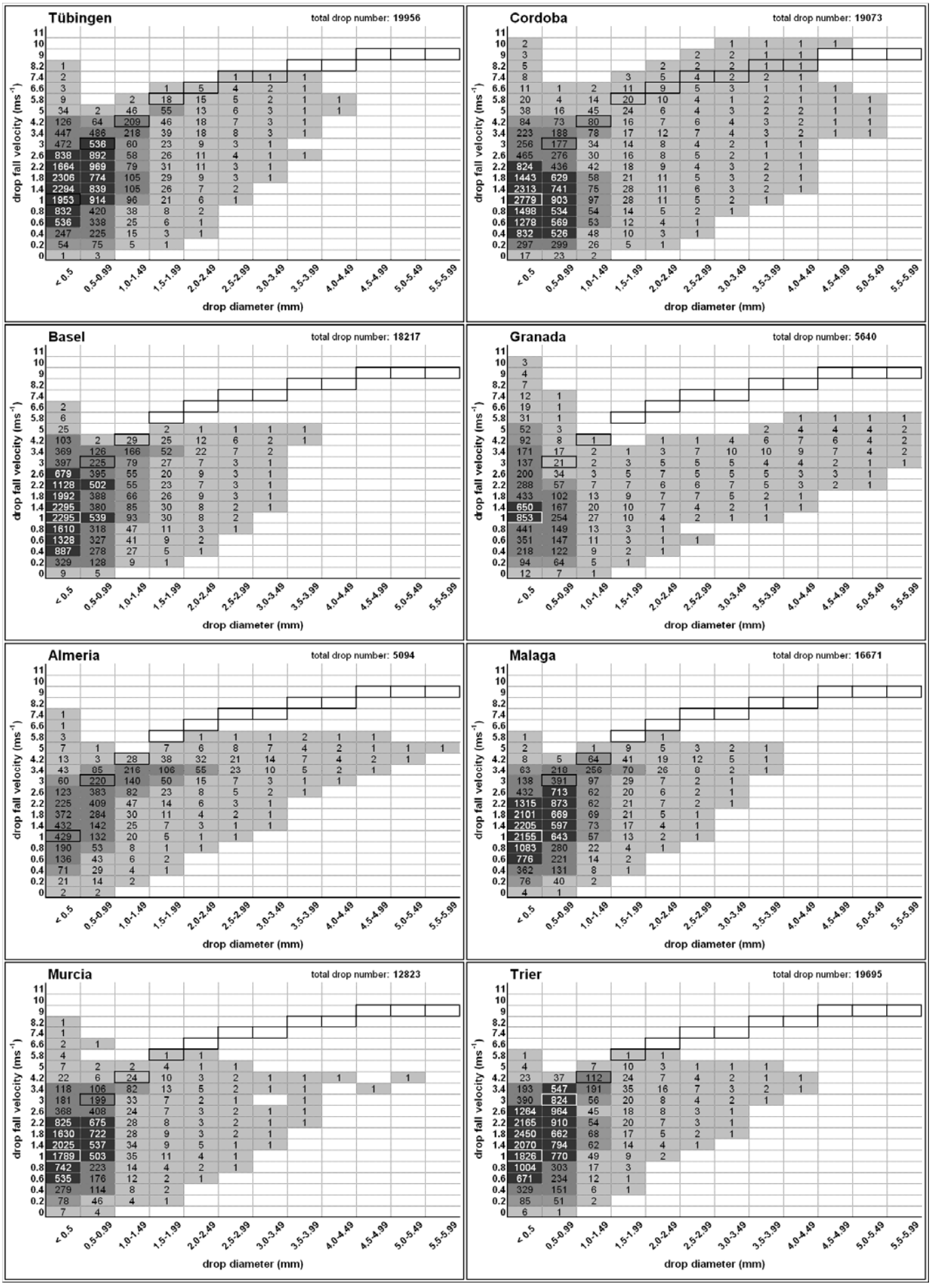
Tübingen
total drop number: 19956
Cordoba
total drop number: 19073
Basel
total drop number: 18217
Granada
total drop number: 5640
Almeria
total drop number: 5094
Malaga
total drop number: 16671
Murcia
total drop number: 12823
Trier
total drop number: 19695
drop fall velocity (ms⁻¹)
drop diameter (mm)
< 0.5
0.5-0.99
1.0-1.49
1.5-1.99
2.0-2.49
2.5-2.99
3.0-3.49
3.5-3.99
4.0-4.49
4.5-4.99
5.0-5.49
5.5-5.99

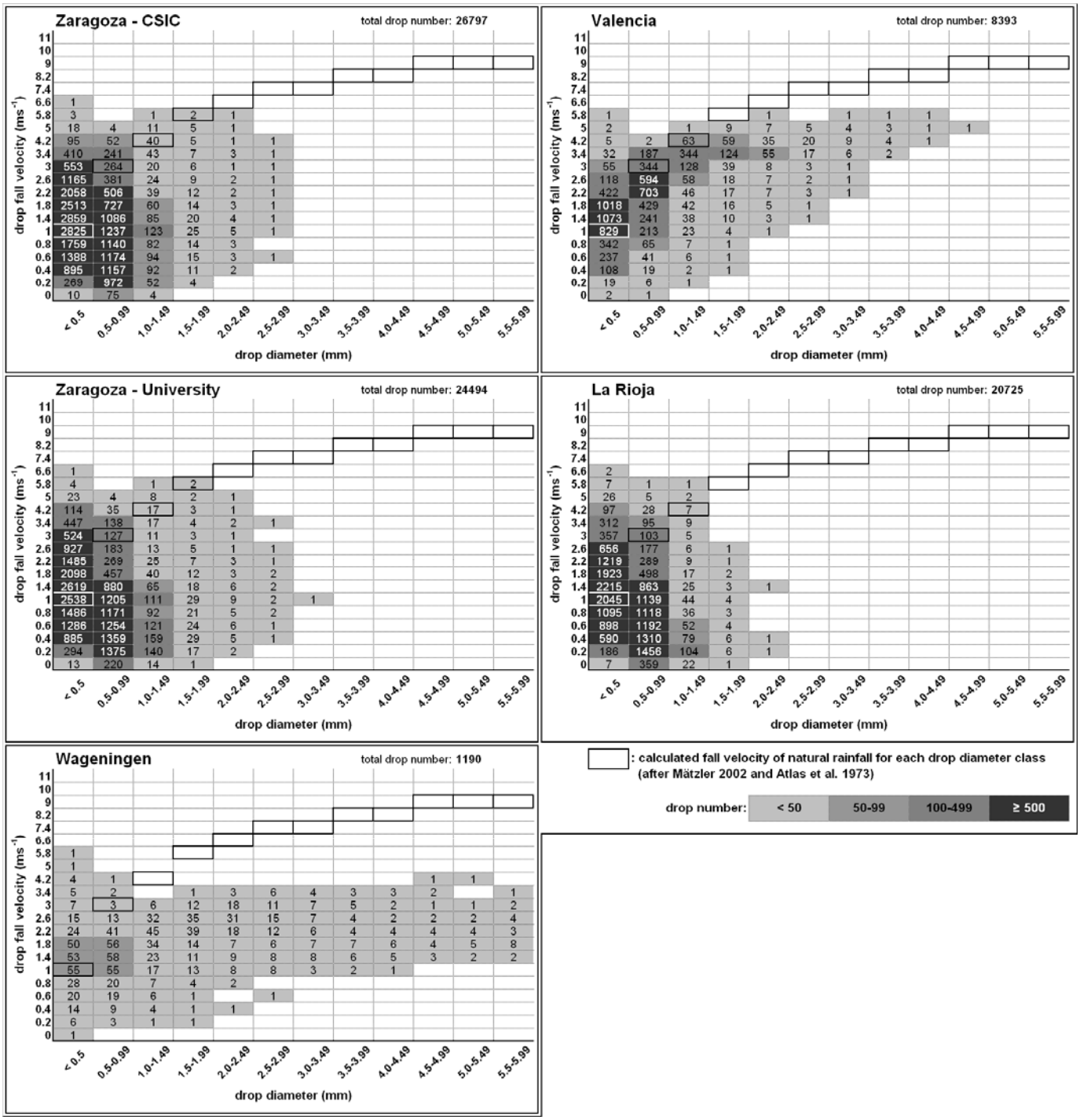


**Fig. 3.** Average drop size distribution and drop fall velocity for each rainfall simulator. Shown are mean values representing 1 min simulated rainfall (n: 25 on five positions [WA: n: 3 on one position]). Each box gives counted total number of drops, fall velocity and drop size class. Calculated drop diameter ranges and corresponding fall velocities for natural rain (Atlas et al., 1973; Mätzler, 2002) are marked with a bold frame.

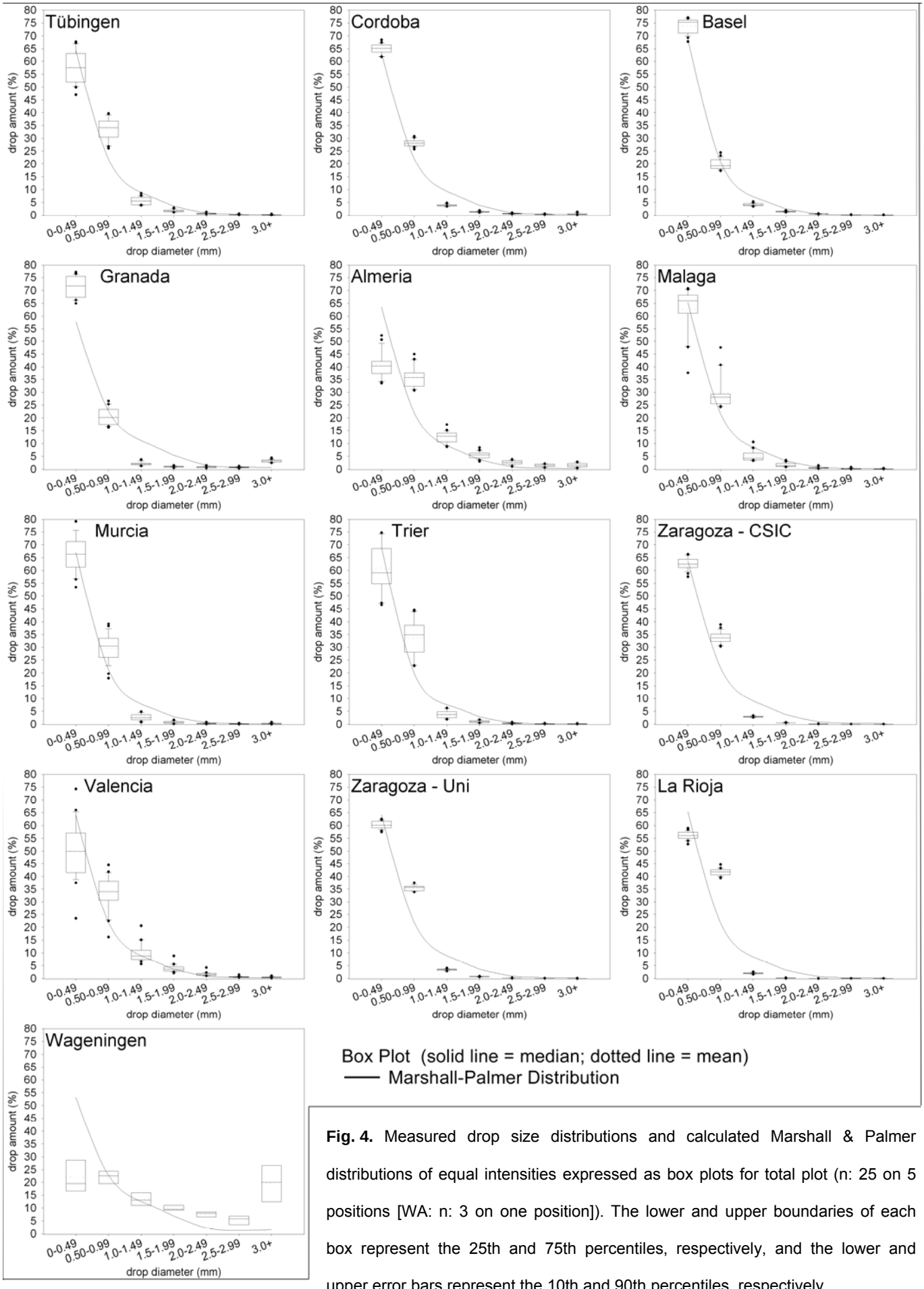


**Fig. 4.** Measured drop size distributions and calculated Marshall & Palmer distributions of equal intensities expressed as box plots for total plot (n: 25 on 5 positions [WA: n: 3 on one position]). The lower and upper boundaries of each box represent the 25th and 75th percentiles, respectively, and the lower and upper error bars represent the 10th and 90th percentiles, respectively.

329

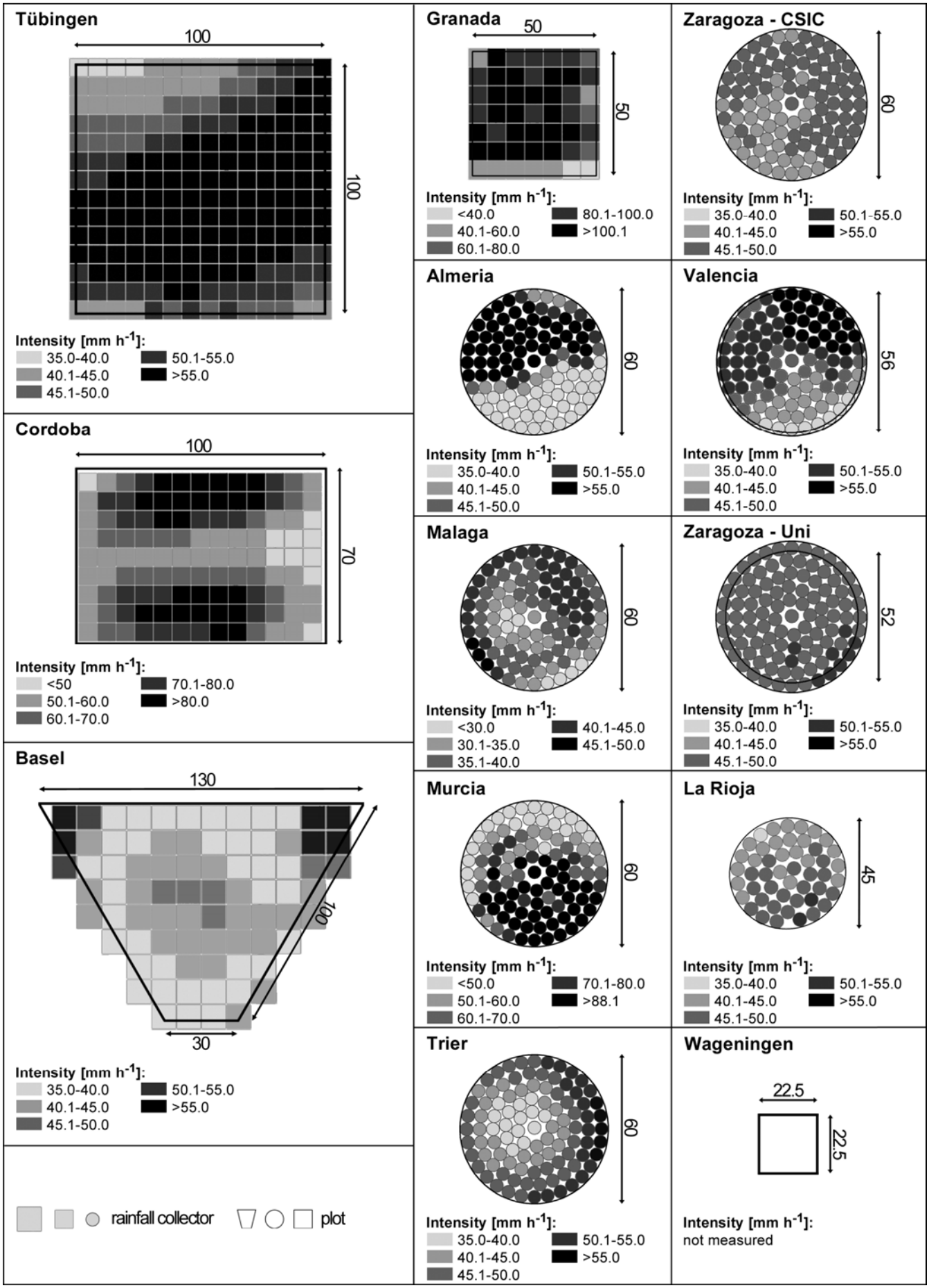


330 **Fig. 5.** Average spatial rainfall distributions for the rainfall simulators (mm $h^{-1}$; n=3 replicates per simulator).

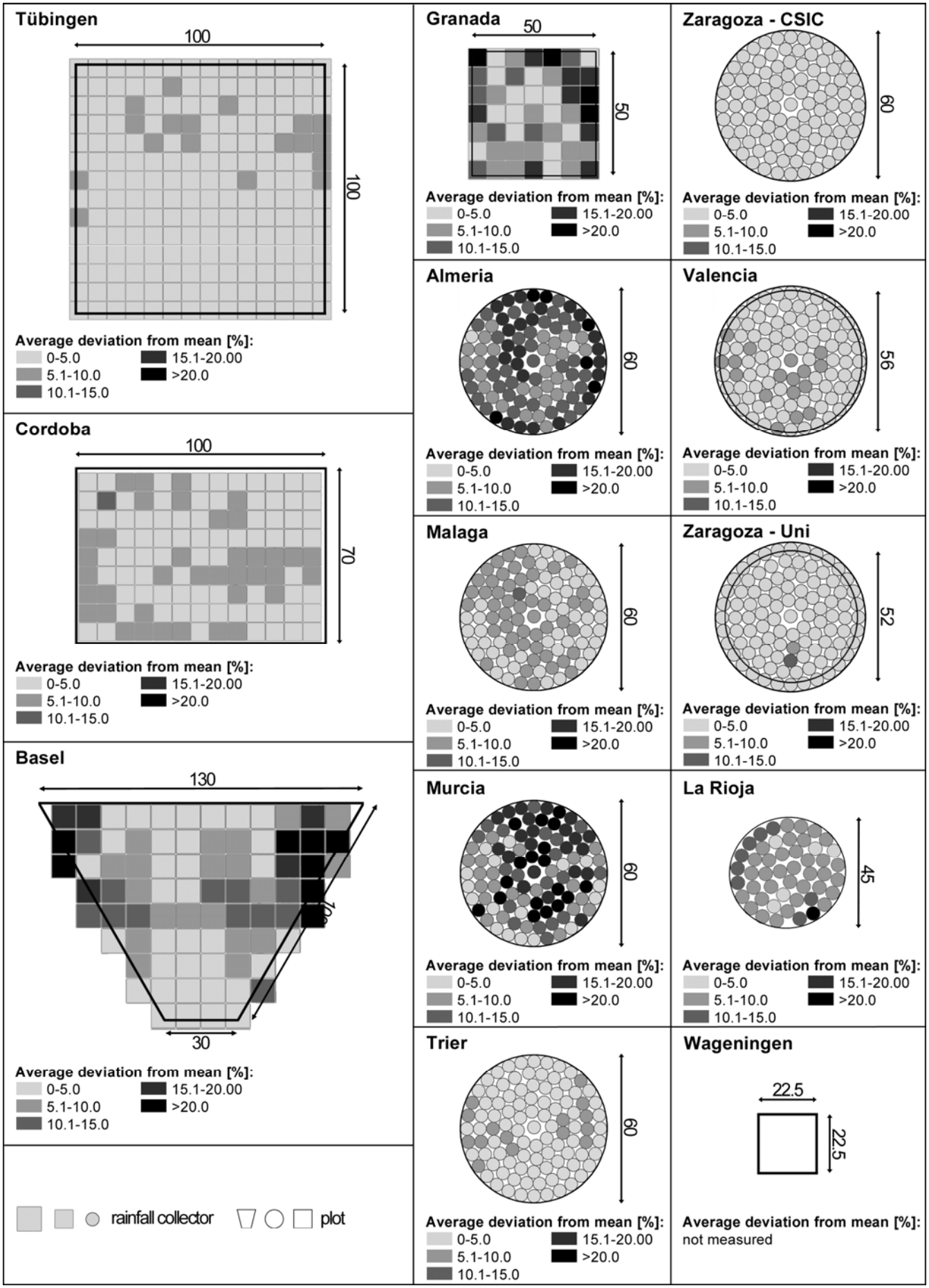


331 **Fig. 6.** Average spatial rainfall variability (%) calculated from 3 replicate measurements for each simulator.

The rainfall simulator from BA produced the highest intensities at the upper left and right corners (51-100 mm $h^{-1}$) and in the middle (45-50 mm $h^{-1}$). The other collectors on the plot showed values between 35 mm $h^{-1}$ and 45 mm $h^{-1}$. The average deviation from the mean was highest at the upper left and right corners, with deviations up to >20%.

The intensities for GR were lowest in the first row directly at the outlet (39-60 mm $h^{-1}$). In contrast, in most of the other collectors across the plot more than twice the amounts (up to 136 mm $h^{-1}$) were measured. The average deviation from the mean showed an almost concentric pattern of rainfall distribution. Central values ranged from 0 to 5% and increased outwards, with values higher than 20% recorded around the edges.

The rainfall simulator from AL produced a spatial rainfall distribution with intensities below 40 mm $h^{-1}$ on the front half of the plot. In contrast, the upper half was characterized by high intensities, most of them >55 mm $h^{-1}$. The average deviation from the mean was 12.8%; many collectors showed deviations >10%, some of them >20%.

The rainfall simulator from MA produced a near concentric pattern of rainfall intensity, with highest intensities (40-50 mm $h^{-1}$) recorded on the right upper area and near the left rim of the plot. The other collectors showed values ranging from 28 mm $h^{-1}$ to 40 mm $h^{-1}$. The plot was evenly covered by collectors with average deviation from the mean values <5% and 5% to 10%.

The intensities generated by MU were higher on the front half (>70 mm $h^{-1}$) of the plot than on the upper half (50-60 mm $h^{-1}$). The average deviation from the mean was similar to the AL plot. Many deviations higher than 15% were recorded across the plot.

The TR-simulator produced a concentric pattern. Lower intensities were measured in the middle (37-45 mm $h^{-1}$); the values increase outwards up to 57 mm $h^{-1}$. Most of the collectors showed an average deviation from the mean of less than 5%, and only a few collectors showed values between 5% and 10%.

The spatial rainfall distribution of the ZAC-simulator can be separated into two parts. In the lower left quarter of the plot, intensities between 40 mm $h^{-1}$ and 45 mm $h^{-1}$ were measured,

359 whereas the other three quarters of the plot recorded intensities of between 45 mm $h^{-1}$ and
360 50 mm $h^{-1}$. The average deviation from the mean for all collectors was less than 5%.
361 The intensities on the plot of the VA-simulator can be separated into three distinct areas. The
362 front area (seen from outlet) was characterized by relatively low intensities that ranged
363 between 35 mm $h^{-1}$ and 45 mm $h^{-1}$. The upper right area recorded intensities up to 55 mm $h^{-}$
364 $^{1}$, and the upper left area recorded values >55 mm $h^{-1}$. The average spatial variability over
365 the three replicates was low; and most of the collectors showed values lower than 5%, with
366 only a few collectors showing values between 5% and 10%.
367 The rainfall simulator from ZAU produced a very uniform intensity distribution. Almost in all of
368 the collectors, intensities between 45 mm $h^{-1}$ and 50 mm $h^{-1}$ were measured. Only in nine
369 collectors, the intensity increased to values ranging between 50 mm $h^{-1}$ and 55 mm $h^{-1}$. With
370 the exception of two collectors, the average deviations from the mean were less than 5%.
371 The simulator used in LR produced a uniform intensity distribution. For almost all of the
372 collectors, intensities between 40 mm $h^{-1}$ and 50 mm $h^{-1}$ were measured. The spatial
373 variability is very heterogeneous across the plot: One collector showed an average deviation
374 from mean higher than 20%, eight collectors recorded values of between 10% and 15%, five
375 collectors between 0 and 5%, and all of the other collectors on the plot showed values
376 between 5% and 10%.
377 Researchers argue (e.g. Esteves et al., 2000; Neff, 1979) that Christiansen Coefficients over
378 80% are essential for rainfall simulation experiments. Most of the simulators meet this
379 requirement, with measured CUs ranging from 60.6% (AL) to 97.8% (ZAU). Additionally, the
380 good reproducibility of the spatial rainfall distribution (max. average deviation from mean over
381 total plot of 13.2%) demonstrates the reproducibility of artificial rainfall of most of the
382 simulators tested.
383
384
385
386

## 4. Conclusions

The comparison of rainfall characteristics provides a good data base for improvements and a consistent picture of the parameters and performance of the simulators can be quantified:

- The use of identical measurement methods provides a means of comparing simulated rainfall characteristics of different simulators.
- The detailed database of artificial rainfall characteristics and the exact knowledge of test conditions represent a prerequisite when assessing erosion, infiltration and runoff results generated during field experiments.
- The LPM is used worldwide for measurements of natural rainfall. This allows detailed comparisons between natural and simulated characteristics in further investigations to be made.
- Kinetic energy values of the simulators are low when compared with values of natural rainfall from literature. Due to the low fall height, it is not possible to reach terminal velocity of large, natural raindrops (large drops are only produced when system pressure and consequently spraying effect are low). This must be taken into account when field results are evaluated.
- All devices investigated are adequate to perform simulations in the field, if all conditions and parameters are well known and accurately controlled.
- Further improvements of individual simulators should concentrate on water efficiency, drop size distribution, spatial rainfall distribution, as well as reproducibility, handling and control of test conditions.

Finally, it can be concluded, that a detailed understanding about relevant features of simulators as well as calibration and test procedure strategies will help to focus results and knowledge, for the purpose of creating a reliable and convincing source of information. Nevertheless, for practical uses, further characteristics of the simulators should be considered e.g. plot size (Iserloh et al., 2013).

**Acknowledgements**

The research for this study was funded by the Deutsche Forschungsgemeinschaft (DFG) project number Ri-835/6-1. We would like to thank the anonymous reviewers for their remarks.

**References**

Abudi, I., Carmi, G., Berliner, P., 2012. Rainfall simulator for field runoff studies. J. Hydrol. 454–455, 76–81.

Adams, J.E., Kirkham, D., Nielsen, D.R., 1957. A portable rainfall-simulator infiltrometer and physical measurements of soil in place. Soil Sci. Soc. Amer. Proc. 21, 473–477.

Alves Sobrinho, T., Gómez-Macpherson, H., Gómez, J.A., 2008. A portable integrated rainfall and overland flow simulator. Soil Use Manage. 24, 163–170.

Angulo-Martínez, M., Beguería, S., Navas, A., Machín, J., 2012. Splash erosion under natural rainfall on three soil types in NE Spain. Geomorphology 175–176, 38–44.

Arnaez, J., Lasanta, T., Ruiz-Flaño, P., Ortigosa, L., 2007. Factors affecting runoff and erosion under simulated rainfall in Mediterranean vineyards. Soil Till. Res. 93, 324–334.

Atlas, D., Srivastava, R.C., Sekhon, R.S., 1973. Doppler radar characteristics of precipitation at vertical incidence. Rev. Geophys.11, 1–35.

Battany, M.C., Grismer, M.E., 2000. Development of a portable field rainfall simulator for use in hillside vineyard runoff and erosion studies. Hydrol. Process. 14, 1119–1129.

Birt, L., Persyn, R., Smith, P., 2007. Technical Note: Evaluation of an Indoor Nozzle-Type Rainfall Simulator. Appl. Eng. Agric. 23, 283–287.

Blanquies, J., Scharff, M., Hallock, B., 2003. The design and construction of a rainfall simulator. In: A gathering of global solutions, proceedings of the 34th annual conference (9pp.). International Erosion Control Association, 24–28 February, Las Vegas, Nevada. Available on-line at: http://www.owp.csus.edu/research/papers/papers/PP044.pdf; accessed 07.08.2012.

Bork, H.R., 1981. Oberflächenabfluss und Infiltration. Ergebnisse von Starkregensimulationen in der Südheide, Ostniedersachsen und in Südost- Spanien. Deutscher Geographentag 43, 159–163.

Boulal, H., Gómez-Macpherson, H., Gómez, J.A., Mateos, L., 2011. Effect of soil management and traffic on soil erosion in irrigated annual crops. Soil Till. Res. 115–116, 62–70.

Bowyer-Bower, T.A.S., Burt, T.P., 1989. Rainfall simulators for investigating soil response to rainfall. Soil Technol. 2, 1–16.

Brandt, C., 1989. The size distribution of throughfall drops under vegetation canopies. Catena 16, 507–524.

453 Brodie, I., Rosewell, C., 2007. Theoretical relationships between rainfall intensity and kinetic
454 energy variants associated with stormwater particle washoff. J. Hydrol. 340, 40–47.

455 Bryan, R., 1974. A simulated rainfall test for the prediction of soil erodibility. Z. Geomorphol.
456 21, 138–150.

457 Calvo, A., Gisbert, B., Palau, E., Romero, M., 1988. Un simulador de lluvia portátil de fácil
458 construcción. In: M. Sala and F. Gallart (Eds.), Métodos y técnicas para la medición
459 de procesos geomorfológicos, Sociedad Española de Geomorfología, Monografía 1,
460 Zaragoza, pp. 6–15.

461 Cerdà, A., 1999. Simuladores de lluvia y su aplicación a la Geomorfología. Estado de la
462 cuestión. Cuadernos de I. Geográfica 25, 45-84.

463 Cerdà, A., Ibànez, S., Calvo, A., 1997. Design and operation of a small and portable rainfall
464 Simulator for rugged terrain. Soil Tech. 11 (2), 161-168.

465 Christiansen, J.E., 1942. Irrigation by Sprinkling. California Agricultural Experiment Station
466 Bulletin 670.

467 Clarke, M.A., Walsh, R.P.D., 2007. A portable rainfall simulator for field assessment of
468 splash and slopewash in remote locations. Earth Surf. Proc. Land. 32, 2052–2069.

469 De Ploey, J., 1981. Crusting and time-dependent rainwash mechanisms on loamy soil. In:
470 Morgan, R.P.C. (Ed.), Soil Conservation, Problems and Prospects. Wiley, pp. 139–
471 154.

472 Disdromet Ltd, Basel, Switzerland, 2001. User Guide for Disdrodata V.1.22.

473 Esteves, M., Planchon, O., Lapetite, J.M., Silvera, N., Cadet, P., 2000. The “EMIRE” large
474 rainfall simulator: design and field testing. Earth Surf. Proc. Land. 25 (7), 681–690

475 Farres, P., 1987. The dynamics of rainsplash erosion and the role of soil aggregate stability.
476 Catena 14, 119–130.

477 Fernández-Gálvez, J., Barahona, E., Mingorance, M.D., 2008. Measurement of Infiltration in
478 Small Field Plots by a Portable Rainfall Simulator: Application to Trace-Element
479 Mobility. Water Air Soil Poll. 191, 257–264.

480 Fister, W., Iserloh, T., Ries, J.B., Schmidt, R.G., 2011. Comparison of rainfall characteristics
481 of a small portable rainfall simulator and a portable wind and rainfall simulator. Z.
482 Geomorphol. 55, 109–126.

483 Fister, W., Iserloh, T., Ries, J.B., Schmidt, R.-G., 2012. A portable wind and rainfall simulator
484 for in situ soil erosion measurements. Catena 91, 72–84.

485 Fornis, R.L., Vermeulen, H.R., Nieuwenhuis, J.D., 2005. Kinetic energy-rainfall intensity
486 relationship for Central Cebu, Philippines for soil erosion studies. J. Hydrol. 300, 20–
487 32.

488 Gunn, R., Kinzer, G.R., 1949. Terminal velocity of water droplets in stagnant air. Journal of
489 Meteorol. 6, 243–248.

490 Hall, M., 1970. Use of the stain method in determining the drop size distribution of coarse
491 liquid sprays. Trans. ASAE 13, 33–37.

Hassel, J., Richter, G., 1988. Die Niederschlagsstruktur des Trierer Regensimulators. Mitteilungen der Deutschen Bodenkundlichen Gesellschaft 56, 93–96.

Hikel, H., Yair, A., Schwanghart, W., Hoffmann, U., Straehl, S., Kuhn, N.J., 2013. Experimental investigation of soil ecohydrology on rocky desert slopes in the Negev Highlands, Israel. Z. Geomorphol. Suppl. 57 (1), 39–58.

Hudson, N., 1963. Raindrop characteristics in south central United States. Rhodesian Journal of Agricultural Research 1, 6–11.

Hudson, N., 1965. The influence of rainfall on the mechanics of soil erosion. M. Sc. Thesis, University of Cape Town, Cape Town, South Africa.

Hudson, N., 1995. Soil Conservation. Batsford Ltd, London, 391 pp.

Humphry, J.B., Daniel, T.C., Edwards, D.R., Sharpley, A.N., 2002. A portable rainfall simulator for plot-scale runoff studies. Appl. Eng. Agric. 18, 199–204.

Imeson, A.C., 1977. A simple field-portable rainfall simulator for difficult terrain. Earth Surf. Processes 2, 431–436.

Iserloh, T., Fister, W., Seeger, M., Willger, H., Ries, J.B., 2012. A small portable rainfall simulator for reproducible experiments on soil erosion. Soil Till. Res. 124, 131–137.

Iserloh, T., Ries, J.B., Cerdà, A., Echeverría, M.T., Fister, W., Geißler, C., Kuhn, N.J., León, F.J., Peters, P., Schindewolf, M., Schmidt, J., Scholten, T., Seeger, M., 2013. Comparative measurements with seven rainfall simulators on uniform bare fallow land. Z. Geomorphol. Suppl. 57 (1), 11–26.

Joss, J., Waldvogel, A., 1967. Ein Spektrograph für Niederschlagstropfen mit automatischer Auswertung. Pure Appl Geophys 68, 240–246.

Kamphorst, A., 1987. A small rainfall simulator for the determination of soil erodibility. Netherlands Journal of Agricultural Science 35, 407–415.

Kincaid, D.C., Solomon, K.H., Oliphant, J.C., 1996. Drop size distributions for irrigation sprinklers. T. ASAE 39, 839–845.

King, B.A., Winward, T.W., Bjorneberg, D.L., 2010. Laser Precipitation Monitor for Measurement of Drop Size and Velocity of Moving Spray-Plate Sprinklers. Appl. Eng. Agric. 26 (2), 263-271.

Lascelles, B., Favis-Mortlock, D.T., Parsons, A.J., Guerra, A.J.T., 2000. Spatial and temporal variation in two rainfall simulators: implications for spatially explicit rainfall simulation experiments. Earth Surf. Proc. Land. 25, 709–721.

Laws, J.O., Parsons, D.A., 1943. The relation of raindrop-size to intensity. Trans. Am. Geophys. Union 24, 452–460.

León, F.J., Echeverría, M.T., Badía, D., Martí, C., Álvarez, C.J., 2013. Effectiveness of wood chips cover at reducing erosion in two contrasted burnt soils. Z. Geomorphol. Suppl. 57 (1), 27–37.

Li, X.-Y., Contreras, S., Solé-Benet, A., Cantón, Y., Domingo, F., Lázaro, R., Lin, H., Van Wesemael, B., Puigdefábregas, J., 2011. Controls of infiltration–runoff processes in Mediterranean karst rangelands in SE Spain. Catena 86, 98–109.

532 Loch, R.J., Robotham, B.G., Zeller, L., Masterman, N., Orange, D.N., Bridge, B.J., Sheridan,
533 G., Bourke, J.J., 2001. A multi-purpose rainfall simulator for field infiltration and
534 erosion studies. Soil Res. 39, 599–610.

535 Luk, S., 1985. Effect of antecedent soil moisture content on rainwash erosion. Catena 12,
536 129–139.

537 Marshall, J.S., Palmer, W.M., 1948. Relation of drop size to intensity. Journal of Meteorol. 5,
538 165-166.

539 Martínez Mena, M., Abadía, R., Castillo, V., Albaladejo Montoro, J., 2001a. Diseño
540 experimental con lluvia simulada para el estudio de los cambios en la erosión del
541 suelo durante la tormenta. Cuaternario y Geomorfología 15, 31–43.

542 Martínez-Mena, M., Castillo, V., Albaladejo, J., 2001b. Hydrological and erosional response
543 to natural rainfall in a semi-arid area of south-east Spain. Hydrol. Process. 15, 557–
544 571.

545 Martínez-Murillo, J.F., Ruiz-Sinoga, J.D., 2007. Seasonal changes in the hydrological and
546 erosional response of a hillslope under dry-Mediterranean climatic conditions (Montes
547 de Málaga, South of Spain). Geomorphology 88, 69–83.

548 Mätzler, C., 2002. Drop-Size Distributions and Mie Computations for Rain. Research Report
549 No. 2002-16. Institut für Angewandte Physik, Uni Bernensis.

550 Medalus, 1993. Medalus II report. Silsoe College, Cranfield University, Silsoe.

551 Meyer, L.D., 1988. Rainfall simulators for soil conservation research. In: Lal, R., (Ed.), Soil
552 Erosion Research Methods. Soil and Water Conservation Society, Ankeny, IO,
553 U.S.A., 75-95.

554 Morgan, R.P.C., Quinton, J.N., Smith, R.E., Govers, G., Poesen, J.W.A., Auerswald, K.,
555 Chisci, G., Torri, D., Styczen, M.E., Folley, A.J.V., 1998. The European Soil Erosion
556 Model (EUROSEM): Documentation and User Guide. Silsoe College, Cranfield
557 University, Silsoe, Bedford.

558 Nadal-Romero, E., Lasanta, T., Regüés, D., Lana-Renault, N., Cerdà, A., 2011. Hydrological
559 response and sediment production under different land cover in abandoned farmland
560 fields in a mediterranean mountain environment. Boletín de la Asociación de
561 Geógrafos Espanoles 55, 303–323.

562 Nadal-Romero, E., Regüés, D., 2009. Detachment and infiltration variations as consequence
563 of regolith development in a Pyrenean badland system. Earth Surf. Proc. Land. 34
564 (6), 824–838.

565 Neal, J.H., 1937. The effect of the degree of slope and rainfall characteristics on runoff and
566 soil erosion. Research Bulletin, Agricultural Experiments Station University of
567 Missouri, Columbia, USA.

568 Neff, E.L., 1979. Why rainfall simulation? Proceedings of Rainfall Simulator Workshop,
569 Tucson, Az. USDA-SEA ARM-W-10, 3–7.

570 Norton, L.D., 1987. Micromorphological study of surface seals developed under simulated
571 rainfall. Geoderma 40, 127–140.

572 Park, S.W., Mitchell, J.K., Bubenzer, G.D., 1980. An analysis of splash erosion mechanics.
573 In: ASAE 1980 Winter Meeting, Paper No.0-2502, p. 27.

574 Poesen, J., Ingelmo Sanchez, F., Mucher, H., 1990. The hydrological response of soil
575 surfaces to rainfall as affected by cover and position of rock fragments in the top
576 layer. Earth Surf. Proc. Land. 15, 653–671.

577 Regmi, T.P., Thompson, A.L., 2000. Rainfall simulator for laboratory studies. Appl. Eng.
578 Agric. 16, 641–652.

579 Regüés, D., Gallart, F., 2004. Seasonal patterns of runoff and erosion responses to
580 simulated rainfall in a badland area in Mediterranean mountain conditions (Vallcebre,
581 southeastern Pyrenees). Earth Surf. Proc. Land. 29, 755–767.

582 Ries, J.B., Iserloh, T., Seeger, M., Gabriels, D., Rainfall simulations - constraints, needs and
583 challenges for a future use in soil erosion research. Z. Geomorphol. Suppl. 57 (1), 1–
584 10.

585 Ries, J.B., Langer, M., 2001. Runoff generation on abandoned fields in the Central Ebro
586 Basin. Results from rainfall simulation experiments. Cuadernos de investigación
587 geográfica 27, 61–78.

588 Ries, J.B., Seeger, M., Iserloh, T., Wistorf, S., Fister, W., 2009. Calibration of simulated
589 rainfall characteristics for the study of soil erosion on agricultural land. Soil Till. Res.
590 106, 109–116.

591 Rose, C.W., 1960. Soil detachment caused by rainfall. Soil Sci. 89, 28–35.

592 Roth, C.H., Meyer, B., Frede, H.-G., 1985. A portable rainfall simulator to study factors
593 affecting runoff, infiltration and soil loss. Catena 12, 79–85.

594 Salles, C., Poesen, J., 1999. Performance of an optical spectro pluviometer in measuring
595 basic rain erosivity characteristics. J. Hydrol. 218, 142–156.

596 Salles, C., Poesen, J., Borselli, L., 1999. Measurement of simulated drop size distribution
597 with an optical spectro pluviometer: sample size considerations. Earth Surf. Proc.
598 Land. 24, 545–556.

599 Schmidt, R.G., 1998. Beobachtung, Messung und Kartierung der Wassererosion. In: Richter,
600 G. (Ed.), Bodenerosion - Analyse und Bilanz eines Umweltproblems. Wiss. Buchges.,
601 Darmstadt, pp. 110–121.

602 Scholten, T., Geißler, C., Goc, J., Kühn, P., Wiegand, C., 2011. A new splash cup to
603 measure the kinetic energy of rainfall. J. Plant Nutr. Soil Sc. 174 (4), 596–601.

604 Thies, 2004. Bedienungsanleitung 021340/07/04 des Laser Niederschlags Monitor
605 5.4110.x0.x00 V1.09.

606 Torri, D., Regüés, D., Pellegrini, S., Bazzoffi, P., 1999. Within-storm soil surface dynamics
607 and erosive effects of rainstorms. Catena 38, 131–150.

608 van Dijk, A.I.J.M., Bruijnzeel, L.A., Rosewell, C.J., 2002. Rainfall intensity–kinetic energy
609 relationships: a critical literature appraisal. J. Hydrol. 261, 1–23.

610 Wiesner, J., 1895. Beiträge zur Kenntnis der tropischen Regens. Math. Naturwiss. Klasse
611 Akad. Wiss. 104, 1397–1434.

612 Wilm, H.G., 1943. The application and measurement of artificial rainfall on types FA and F
613 infiltrometers. Trans. Am. Geophys. Union 3, 480–484.

614 Wischmeier, W.H., Smith, D.D., 1978. Predicting rainfall erosion losses - A guide to
615 conservation planning. In: USDA Agricultural Research Service Handbook 537.

616 Zhao, Y., Hirschi, M.C., Cooke, R.A., Mitchel, J.K., Ni, B., 1996. Measurement of simulated
617 rainfall characteristics for raindrop erosion studies. ASAE Paper 96-2117, St. Joseph,
618 Mich.